A Nonlinear Model For Harmonic Drive Friction And Compliance

H.D. Taghirad† and P.R. Bélanger‡
Center for Intelligent Machines,
Department of Electrical Engineering,
McGill University, Montréal, H3A 2A7
† taghirad@cim.mcgill.ca, ‡ pbelange@fgsr.lan.mcgill.ca

Abstract—
Despite widespread industrial application of harmonic drives, mathematical representation of their dynamics has not been fully addressed. In this paper a systematic way to capture and rationalize the dynamic behavior of the harmonic drive systems is developed. Simple and accurate models for compliance, hysteresis, and friction are proposed, and the model parameters are estimated using least–squares approximation for linear and nonlinear regression models. A statistical measure of variation is defined, by which the reliability of the estimated parameter for different operating condition, as well as the accuracy and integrity of the proposed model is quantified. By these means, it is shown that a linear stiffness model best captures the behavior of the system when combined with a good model for hysteresis. Moreover, the frictional losses of harmonic drive are modelled at both low and high velocities. The model performance is assessed by comparing simulations with the experimental results on two different harmonic drives. Finally, the significance of individual components of the nonlinear model is assessed by a parameter sensitivity study using simulations.

I. Introduction

Developed in 1955 primarily for aerospace applications, harmonic drives are high–ratio and compact torque transmission systems. Harmonic drive transmission employs a non-rigid gear called *flexspline* for speed reduction. As a consequence, the transmission stiffness is lower than that in conventional transmissions. Furthermore, the nonlinear relation between the input and the output torques makes it more challenging to control the system. Following this impetus for investigation, several researchers have made valuable contributions to the technological status and control of harmonic drive systems. The Russians were perhaps the first to initiate substantial research on the dynamic behavior of harmonic drives [1], [16], [10]. More recently Tuttle and Seering devoted an extensive effort to model the stiffness, positioning accuracy, gear tooth-meshing mechanism and friction of harmonic drives [24]. Their experimental observations show that the velocity response to step commands in motor current are not only contaminated by serious vibration, but also by unpredictable jumps. The velocity response observations were used to guide the development of a series of models with increasing complexity for harmonic drive behavior. Their most complex model involve kinematic error, nonlinear stiffness, and gear-tooth interface with frictional losses.

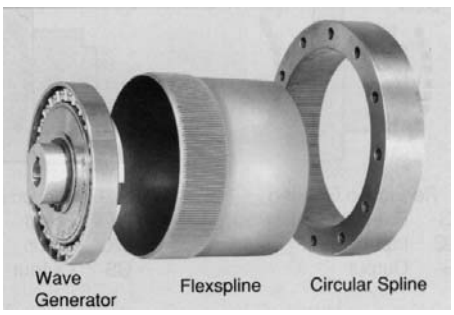

Fig. 1. Harmonic drive components

Kircanski and Goldenberg have also attempted to model the harmonic drive in detail [11]. They used the drive system in contact with a stiff environment, as opposed to the free–motion experiments used by Tuttle and Seering [24]. They illustrated that for their case, nonlinear stiffness, hysteresis and friction are more tractable. Simple models for soft-windup, hysteresis and friction were proposed and the parameters were identified by restrained motion experiments.

Hsia [8], Legnani [12], Marilier [14], Chedmail et al. [5] and Seyfferth [15] are among others who attempted to model the stiffness, friction and position accuracy of harmonic drive systems. All these researchers noted the inherent difficulties in finding an accurate model for the system.

In this paper a moderately complex model of harmonic drive system is developed. Constrained and free motion experiments are use to identify the model parameters and illustrate the fidelity of the model for two different types of harmonic drive systems. It is shown that a linear stiffness model for stiffness combined with a velocity dependent structural damping model can replicate the hysteresis torsion curve of the system for restrained motion experiments. The frictional losses of the transmission has been modelled using Coulomb friction, Viscous damping and Stribeck friction. Both high speed, and low speed friction terms has been identified using free and constrained motion experiments respectively. Finally, the simulation of the system built in Simulink has been used to verify the model by experiments. It has been verified that the simulation accurately predicts the experiments.

II. Experimental Setup

Two harmonic drive testing stations were used to monitor the behaviour of two different harmonic drives. In

both setups the harmonic drive is driven by a DC motor, and a load inertia is used to simulate the robot arm for free–motion experiments. Also a positive locking system is designed such that the output load can be locked to the ground. In the first setup, a brushed DC motor from Electro–Craft, model 586-501-113, is used. Its weight is 1.36 Kg, with maximum rated torque of 0.15 Nm, and torque constant of 0.0543 Nm/amp. The servo amplifier is a 100 Watts Electro–Craft power amp model Max-100-115. The harmonic drive in this setup is from RHS series of HD systems model RHS-20-100-CC-SP, with gear ratio of 100:1, and rated torque of 40 Nm. In the second setup the DC motor is a brushless Kollmorgen Inland motor, model RBE-01503-A00. Its weight is 475 gr, with maximum rated torque of 5.6 Nm, and torque constant of 0.1815 Nm/amp. The servo amplifier is a FAST Drive Kollmorgen, model FD 100/ 5E1. The harmonic drive is from CFS series of HD Systems, Inc. with gear ratio 160:1, and rated peak torque of 178 Nm.

In the first experimental setup, the circular spline is fixed to the ground and the output is carried by the flexspline, while in the other setup, the flexspline is fixed and the circular spline is used for output rotation. By this arrangement, the behavior of the transmission under different operating configurations can be examined. Each setup is equipped with a tachometer to measure the motor velocity, and an encoder on the load side to measure the output position. The output torque is measured by a Wheatstone bridge of strain gauges mounted directly on the flexspline [21], and the current applied to the DC motor is measured from the servo amplifier output. These signals were processed by several data acquisition boards and monitored by a C-30 Challenger processor executing compiled computer C codes [17].

III. Modelling and Identification

The goal of modelling the harmonic drive system is to discover the simplest representation which can replicate system performance to a desired level of accuracy. Our purpose in modelling is to implement a model–based torque control algorithm on the system. Moreover, we used the computer model for examining and improving control laws, before implementing them. As recommended by other researchers [11], [24], in order to comply this objective it is necessary to have at least a simple and accurate model for friction, and compliance of harmonic drive systems. In practice it has been proven that the knowledge obtained through the process of modelling and identification of the system becomes a powerful medium for understanding, and improving the design, as well as for providing new horizons for controller design [19], [20].

A complete model of harmonic drive includes the frictional losses and compliance effect in addition to the reduction property of the transmission. Figure 2 represents a complete model of the system, in which the friction losses are separated into the wave generator bearing friction T_{f_1}, gear meshing friction T_{f_2}, output bearing friction T_{f_3} and

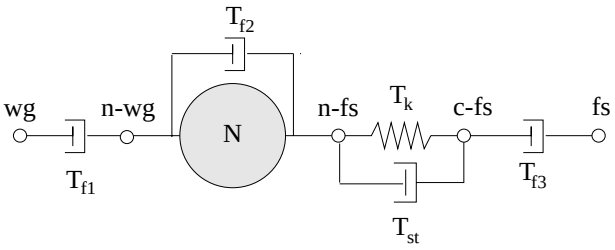

Fig. 2. Transmission model of the harmonic drive with compliance and friction

the flexspline structural damping T_{st}, while T_k represents the stiffness of the flexspline. The position and torque balance between each two nodes can be represented by the following equations:

$$\begin{cases} \theta_{wg} = \theta_{n_{wg}} \\ T_{wg} = T_{n_{wg}} + T_{f_1} \end{cases} \quad (1)$$

$$\begin{cases} \theta_{n_{wg}} = N \cdot \theta_{n_{fs}} \\ T_{n_{wg}} = \frac{1}{N} T_{n_{fs}} + T_{f_2} \end{cases} \quad (2)$$

$$\begin{cases} T_{n_{fs}} = T_{c_{fs}} \\ T_{n_{fs}} = T_k + T_{st} \end{cases} \quad (3)$$

$$\begin{cases} \theta_{c_{fs}} = \theta_{fs} \\ T_{fs} = T_{c_{fs}} - T_{f_2} \end{cases} \quad (4)$$

The compliance model relates the stiffness T_k and structural damping T_{st} to the relative torsion of the flexspline $\Delta\theta = \theta_{n_{fs}} - \theta_{c_{fs}}$. The following Sections III-A, and III-B elaborate our proposed model for compliance, and friction respectively.

A. Harmonic Drive Compliance

As described in the manufacturer's catalogue [9], a typical shape of the harmonic drive compliance curve is as the experimental result of Figure 3. This curve illustrates harmonic drive nonlinear stiffness and hysteresis. To capture the nonlinear stiffness behavior, manufacturers suggest using piecewise–linear approximations [9], whereas other researchers prefer a cubic polynomial approximation [24], [25]. The hysteresis effect, however, is more difficult to model, and consequently it is often ignored. Recently Seyfferth et al. proposed a fairly complex model to capture the hysteresis [15]. The hysteresis in the harmonic drive compliance profile is caused by structural damping of the flexspline. The inherent coupling of stiffness torque and structural damping, therefore, makes it very hard to identify those separately.

We suggest that Figure 3 is in fact a Lissajous figure, and that we identify both the stiffness and damping of the flexspline together using least–squares estimation. By means of least square estimation, for each experiment a set of parameters is obtained. However, these parameters are deemed acceptable, only if they are consistent for other experiments. By consistency we mean a statistical measure, namely *the ratio of the standard deviation to the average value of each parameter estimated for different experiments.*

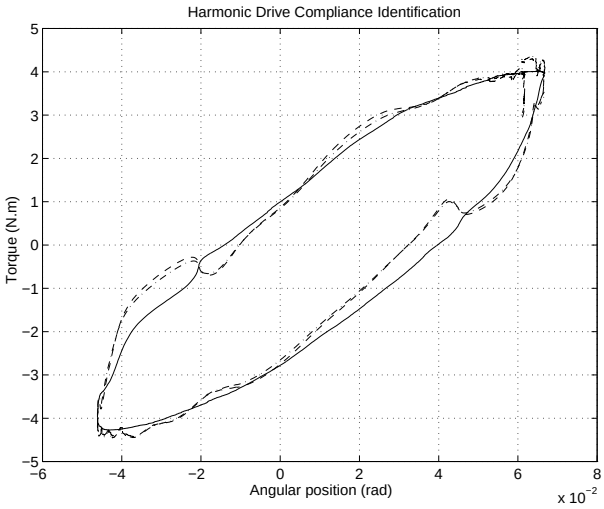

Fig. 3. Typical hysteresis curve and its model for optimal α (dash-dot), and $\alpha = \frac{1}{2}$ (dashed)

TABLE I
HARMONIC DRIVES ESTIMATED PARAMETERS

	Harmonic Drive 1		Harmonic Drive 2	
	Estimated Parameter	Consist. Measure	Estimated Parameter	Consist. Measure
α	$\frac{1}{2}$	0%	$\frac{1}{2}$	0%
K_1	6340	9.6%	104.2	4.36%
T_{st}	57.2	28.2%	7.96	28.0%
J_{eff}	1.0×10^{-4}	6.38%	1.0×10^{-4}	8.72%
T_{v_p}	3.7×10^{-4}	16.7%	1.8×10^{-3}	13.2%
T_{v_n}	3.5×10^{-4}	19.3%	2.1×10^{-3}	8.42%
T_{s_p}	4.6×10^{-2}	23.7%	7.5×10^{-2}	29.2%
T_{s_n}	4.4×10^{-2}	24.0%	3.3×10^{-2}	30.8%
$T_{ss_{p1}}$	-0.0076	14.7%	-0.0487	20.3%
$T_{ss_{n1}}$	-0.0203	23.8%	-0.0450	18.6%
T_{ss_2}	0.1	0%	0.1	0%

If this measure is small, we have a good consistency for different experiments, and in other words, the model is good enough to capture the dynamics of the system. It has been verified by simulations that having consistency measure less than 30% gives a relatively good match to the experiments [18].

Linear and cubic models for compliance and many different models for structural damping were tried in this framework. The Dahl model for friction [6], [22] and the Duham, Preisach and Babuska models for hysteresis [13], are among the many dynamic models used to replicate the hysteresis torsion curve. The details of these dynamic models and their identification results are elaborated in [18]. We observed, however, that a linear stiffness model accompanied with a static model which relates the structural damping to a power of the velocity, can best capture hysteresis behavior. The reason why dynamic models were not capable of accurately predicting hysteresis in harmonic drive structural damping is that despite their dynamic relation, the dependence of the structural damping torque to a power of the velocity was not accommodated. Hence, our proposed model, simpler in structure, appears to better characterize the hysteresis. In practice the consistency measure of identified parameters in our model is much less than those of other dynamic models we examined.

Equation 5 gives in detail the compliance model, where $\Delta\theta$ is the flexspline relative torsion.

$$T_{meas} = K_1 \Delta\theta + T_{st} |\Delta\dot{\theta}|^{\alpha} \text{sign}(\Delta\dot{\theta}) \tag{5}$$

To identify the model parameters, a set of constrained motion experiments has been employed, in which the torque T_{meas} and the motor velocity have been measured. The experiment shape functions are the same as that explained in DC motor experiments. Equation 5 forms a nonlinear regression in which K_1, T_{st} and α are unknown. Using an iterative least–squares solution for this nonlinear regression model, it is found that the optimal estimate of α is very close to 0.5. Consequently the structural damping can be related to the square root of the relative torsion velocity. Figure 3 illustrates a typical hysteresis torsion curve fitted by the model, comparing the difference between the optimal α and $\alpha = \frac{1}{2}$. The maximum mismatch (points $(-2, -0.5)$ and $(0.5, 0.8)$ in Figure 3) occurs when the velocity is changing rapidly; otherwise, the model is approximating the hysteresis curve quite accurately. By fixing the value of $\alpha = \frac{1}{2}$, Equation 5 forms a linear regression model for the system and can be solved for different experiments. Table I summarizes the compliance parameter for the harmonic drives of our two setups.

B. Harmonic Drive Friction

All harmonic drives exhibit power loss during operation due to transmission friction. Figure 2 illustrates the schematics of the harmonic drive model. The bulk of energy dissipation can be blamed on the wave generator bearing friction T_{f_1}, gear meshing friction T_{f_2}, output bearing friction T_{f_3} and the flexspline structural damping T_{st}. Among them, most of the frictional dissipation results from gear meshing. Also comparing the ball–bearing frictions, T_{f1} is more important than T_{f_3} since it is acting on the high speed/low torque port of transmission, and its effect on the dynamics of the system is magnified by the gear ratio. The transmission torque is measured directly by strain gauges mounted on the flexspline (namely node c_{fs} of Figure 2). The torque balance, therefore, can be written as:

$$T_{wg} = \frac{1}{N}(T_{meas}) + T_{f_1} + T_{f_2} \tag{6}$$

in which the measured torque $T_{meas} = T_k + T_{st}$, N is the gear ratio, and T_{wg} is the resulting torque of the wave generator, provided by the DC motor. T_{wg} can be related to the input current by [17]:

$$T_{wg} = K_m i - J_m \ddot{\theta} - T_{f_m} \tag{7}$$

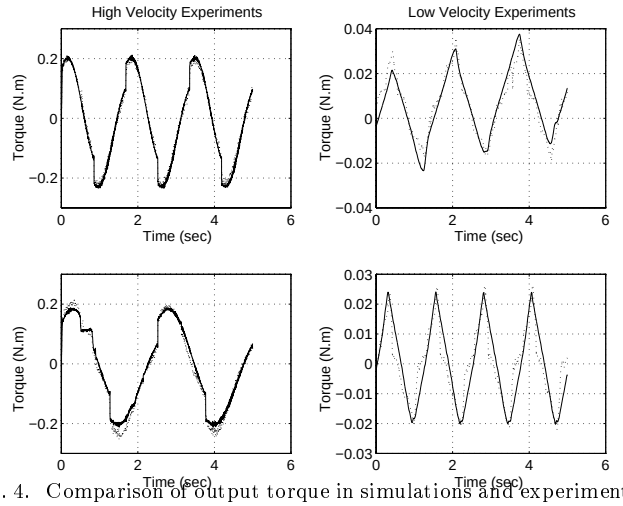

Fig. 4. Comparison of output torque in simulations and experiments; dotted: experiment, solid: simulation

Thus, the final torque balance of the system is the following:

$$K_m i - \frac{1}{N} T_{meas} = J_{eff} \ddot{\theta}_{wg} + (T_{f_m} + T_{f_1} + T_{f_2}) \qquad (8)$$

in which K_m is the motor torque constant, J_{eff} is the effective input inertia, and T_{f_m} is the motor friction. The gear meshing friction torque is modelled as Coulomb, viscous and Stribeck friction [3], [23], having velocity–direction–dependent coefficient. This can be represented by:

$$\begin{aligned} &T_{f_2} = T_{v_p} \dot{\theta}_{wg}\ u_{-1}(\dot{\theta}_{wg}) + T_{v_n} \dot{\theta}_{wg}\ u_{-1}(-\dot{\theta}_{wg}) + \\ &T_{s_p} \mathrm{sign}(\dot{\theta}_{wg})\ u_{-1}(\dot{\theta}_{wg}) + T_{s_n} \mathrm{sign}(\dot{\theta}_{wg})\ u_{-1}(-\dot{\theta}_{wg}) + \\ &T_{ss_{p1}} \mathrm{sign}(\dot{\theta}_{wg})\ u_{-1}(\dot{\theta}_{wg}) e^{-\left(\frac{\dot{\theta}_{wg}}{T_{ss_{p2}}}\right)^2} + \\ &T_{ss_{n1}} \mathrm{sign}(\dot{\theta}_{wg})\ u_{-1}(-\dot{\theta}_{wg}) e^{-\left(\frac{\dot{\theta}_{wg}}{T_{ss_{n2}}}\right)^2} \end{aligned} \qquad (9)$$

where

$$u_{-1}(x) = \begin{cases} 1 & \text{if } x > 0 \\ 0 & \text{if } x \leq 0 \end{cases} \qquad (10)$$

The Stribeck model for friction can capture the dynamics of the friction at low velocities. Unlike compliance identification, both constrained and free motion experiments are employed to identify the friction model parameters. Free–motion experiments are suitable for viscous and Coulomb friction, while constrained–motion experiments operate the system at low velocities which are ideal for Stribeck coefficient identification. Free motion low–velocity experiments are used as well, for Stribeck coefficient identification. The experiment inputs are the same as that explained in DC motor experiments, where for constrained motion case 20 experiments, and for free motion case 30 experiments are considered for each setup.

Equation 8 forms a linear regression model for the high velocity experiments in the absence of the nonlinear Stribeck terms. Viscous and Coulomb friction coefficients $T_{v_p}, T_{v_n}, T_{s_p}$ and T_{s_n}, and the inertia J_{eff} is obtained from least-Squares solution to this case. For low–velocity experiment also, Equation 8 can provide a linear regression if $T_{ss_2} = T_{ss_{p2}} = T_{ss_{n2}}$ is assumed to be known. Table I summarizes the estimated friction parameters of two harmonic drives, and their consistency measure and Figure 4 illustrates the output torque fit obtained by the model for four typical experiments, assuming fixed $T_{ss_2} = 0.1$. The consistency measure for all parameters are less than 30%, which indicates the reliability of the estimated parameters. It should be noted that in this regression model instead of the internal system friction T_{f_m}, T_{f_1} and T_{f_2}, the entire friction of the system ($T_f = T_{f_m} + T_{f_1} + T_{f_2}$), can be identified. This imposes no limitation on the identification procedure, since only the entire friction T_f is required for the simulations.

It is important to note that the estimated Stribeck friction coefficients are negative, which is in contrary to the usual dynamics of friction reported at low velocities [2], [7]. Nevertheless, this represents rising friction in harmonic drives at low velocities and no stiction, verifying the manufacturers claim [4]. This may be rationalized by the fact that the main bulk of frictional losses in the harmonic drive systems are due to the gear meshing but that, contrary to other transmissions, a combination of elastic deformation of the flexspline and gear teeth engagement contributes to the velocity reduction. Therefore, the low–velocity experiments in the harmonic drive transmission shows smoother startup velocity when compared to other transmissions. This is verified by both constrained and unconstrained motion experiments, where no stick–slip or stiction is observed. The reliability of the negative Stribeck coefficient is assessed first by the acceptable consistency measure for the Stribeck coefficients, and second by the similar results obtained for the two different harmonic drives.

IV. Modelling and Identification Verification

To verify the validity of the modelling scheme, simulations of the system under constrained and free–motion cases are developed in the Simulink. The equation of motion for each component of the system is integrated into a simulation unit, and the simulation is initialized by downloading the identified parameters. In order to compare the simulation result of the integrated system to the experiments, an experiment data file is also downloaded into the simulation environment. Hence, using measured DC motor current of a typical experiment as an input to the simulation, the velocity and torque output of the simulated system are compared to that of the experiment. By this means the ability of the simulation to predict the dynamic behaviour of the system is studied.

The output velocity and torque of the simulated system are compared to typical experimental outputs in Figure 5. First the experimental signals are filtered using a fifth–order zero–phase distortion Butterworth filter. Therefore, the torque ripples in free motion experiments, and the noise on the measured velocity in constrained–motion experiments are not displayed in Figure 5. For the system under free–motion, there is an almost perfect match for the velocity, and a relatively good match for the torque curves.

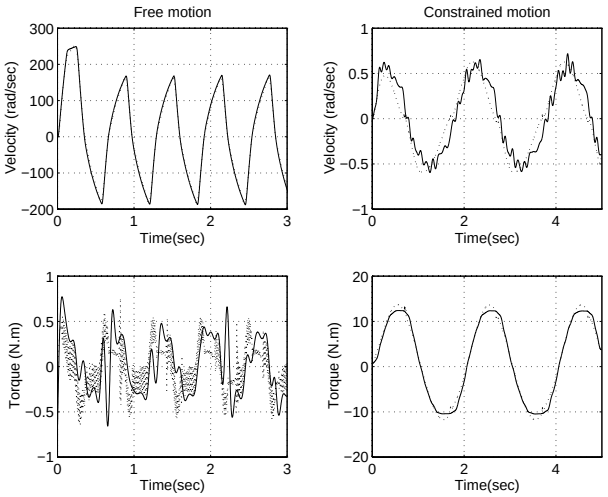

Fig. 5. Simulation verification for system under free and constrained–motion; Solid : Experiment, Dotted : Simulation

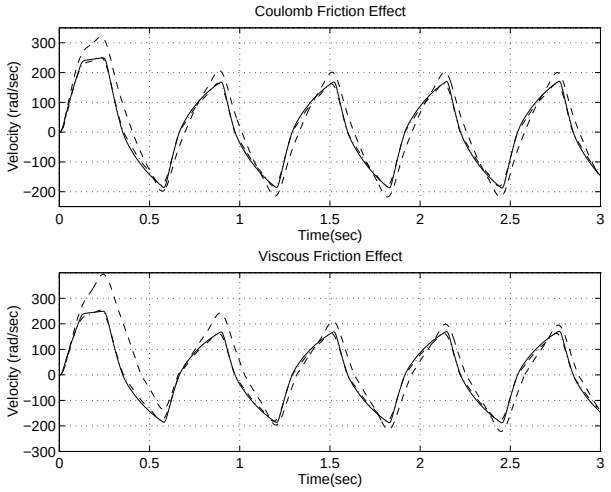

Fig. 6. Comparison of the experiment with the complete and simplified models; Solid : Experiment, Dash-dotted : Complete model, Dashed : Simplified model

The perfect match between the simulation and experiment velocity indicates the ability of the simulation to predict the dynamic behavior of the system. Some oscillations are observed in the simulated torque of the system which are absent in the filtered experimental torque displayed in Figure 5. The measured torque however, displays similar oscillation (torque ripples), but with larger amplitude. It should be mentioned that to have a model for accurate prediction of the torque ripples requires a complex gear meshing mechanism modelling, [24], which is not pursued in this research. Instead, as elaborated in [21], a Kalman filter is employed to estimate the torque ripples, using simple harmonic oscillator model. Despite the simple model used for the prediction, it is shown that Kalman filter can accurately estimate the torque ripples.

For the system under constrained motion, the match between velocities is less accurate compared to that for the free motion system, because of the smaller velocity signal and hence smaller signal–to–noise ratio. However, the resulting torques are quite similar and there is no torque ripple observed for the constrained system. This accurate match was verified for more than twenty disparate experiments for both harmonic drive testing stations. Extensive results are provided for both constrained– and free–motion experiments in [17]. The accurate match between simulation and experiment for different operating ranges indicates the fidelity of the model to accurately predict the dynamic behavior of the system and confirms the effectiveness of modelling and parameter identification schemes to capture the dynamics of the harmonic drive systems.

V. Parameter Sensitivity Study

The significance of individual components of the nonlinear model is assessed by a parameter sensitivity study using simulations. In this study, the simulation results of the complete model and a series of simplified models are compared to the experiments. To examine the effect of Coulomb and viscous friction, the free–motion simulation of the system is employed. For a simplified model, either the Coulomb or the viscous friction coefficient is set to zero, and the simulation results of the complete and simplified model are compared to the experiment. Figure 6 illustrates the comparison results for a typical experiment. In absence of either Coulomb or viscous friction the model is not capable of accurately estimating the experimental result. Hence, we may conclude that accurate identification of Coulomb and viscous friction coefficients significantly contributes to the accuracy of the simulations. Stribeck friction, however, is only present in very low–velocity experiments, and its effect in the typical experiment of Figure 6 is negligible. However, in applications where fine motions at low velocities are demanded, modelling and identification of Stribeck friction is prominent.

To examine the effect of the compliance model the constrained–motion simulation of the system is employed. For simplified models first the stiffness is reduced by one

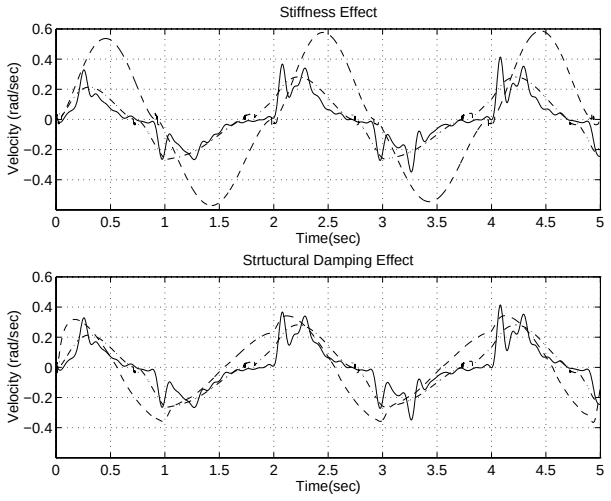

Fig. 7. Comparison of the experiment with the complete and simplified models; Solid : Experiment, Dash-dotted : Complete model, Dashed : Simplified model

order of magnitude, and then the structural damping coefficient is set to zero, while keeping all the other identified parameters of the model. Figure 7 illustrates the comparison results of the complete and simplified models to the experiment. It is observed in this figure that the lack of accuracy in identifying the stiffness parameter results in larger velocity amplitude in the simulations. Furthermore, an inaccurate structural damping coefficient results in phase estimation error of the velocity. Therefore, both stiffness and structural damping estimation contribute significantly into accuracy of the model.

VI. Conclusions

Based on experimental and theoretical studies, a systematic way to capture and rationalize the dynamics of the harmonic drive systems is introduced. Simple and accurate models for compliance, hysteresis, and friction are established and model parameters are identified using least–squares approximation. A measure of consistency is defined, by which the reliability of the estimated parameter for different operating condition, as well as the accuracy of the simple model is quantified. From compliance modelling results, it has been shown that identifying stiffness and structural damping together will resolve the reported difficulties in determining the compliance parameters. Moreover, it has been shown that a linear stiffness model best captures the behavior of system when combined with a good model for hysteresis. A simple static model for hysteresis is also introduced, and it is shown that this simple model can replicate the hysteresis effect in harmonic drives better than some other more complex dynamic models reported in the literature. Friction losses of the harmonic drive are modelled at both low and high velocities. From experiments on two different harmonic drives it is observed that there is no stiction in the transmission, but rather a rising friction acts at low velocities.

The model performance is assessed by a simulation verifying the experimental results for both constrained– and free–motion cases.The simulated velocity and torque of the system is compared to experimental results for several constrained– and free–motion experiments. An accurate match between simulation and experiment for different operating ranges are obtained, which indicates the fidelity of the model to accurately predict the dynamic behavior of the system. Moreover, it confirms the effectiveness of modelling and parameter identification schemes to capture the dynamics of the harmonic drive systems. Furthermore, the significance of individual components of the nonlinear model is assessed by a parameter sensitivity study. By comparing the simulation results of the complete model and a series of simplified models to the experiment results, it is concluded that accurate estimation of Coulomb and viscous friction significantly contributes to the accuracy of the simulations. Finally, it is shown that both stiffness and structural damping are prominent for the accuracy of the constrained–motion simulations.

References

[1] N.A. Aliev. A study of the dynamic behavior of flexible gears in harmonic drives. *Soviet Engineering Research*, 66(6):7–11, 1986.

[2] B. Armstrong-Helouvry. Stick slip and control in low speed motion. *IEEE Transactions on Automatic Control*, 38(10):1483–1496, October 1993.

[3] B. Armstrong-Helouvry, P. Dupont, and C. Canudas de wit. A survey of models, analysis tools and compensation methods for control of machines with friction. *Automatica*, 30(7):1083–1138, 1994.

[4] J.H. Charlson. Harmonic drives for servomechanisms. *Machine design*, 57(1):102–106, January 1985.

[5] P. Chedmail and J.P. Martineau. Characterization of the friction parameters of harmonic drive actuators. *International Conference on Dynamics and Control of Structures in Space*, 1:567–581, 1996.

[6] P.R. Dahl. Solid friction damping of mechanical vibration. *AIAA Journal*, 14(12):1675–1682, December 1976.

[7] D.P. Hess and A. Soom. Friction at a lubricated line contact operating at oscillating sliding velocities. *Journal of Tribology*, 112(1):147–152, January 1990.

[8] L. Hsia. The analysis and design of harmonic gear drives. *Proceedings of the 1988 IEEE International Conference on Systems, Man and Cybernetics*, 1:616–619, 1988.

[9] HD Systems Inc. *Harmonic drive gearing*. Manufacturer's Cataloge, 1991.

[10] M.N. Ivanov. *Harmonic Gear Transmissions*. Visshaya shkola, M., (Russian), 1981.

[11] N. Kircanski, A. Goldenberg, and S. Jia. An experimental study of nonlinear stiffness, hysteresis, and friction effects in robot joint with harmonic drives and torque sensors. *Proceedings of the Third International Symposium on Experimental Robotics*, 1:147–154, 1993.

[12] G. legnani and R. Faglia. Harmonic drive transmission: the effect of their elasticity, clearance and irregularity on the dynamic behaviour of an actual scara robot. *Robotica*, 10:369–375, October 1992.

[13] J.W. Macki, P. Nistri, and P. Zecca. Mathematical models for hysteresis. *SIAM Review*, 35(1):94–123, March 1993.

[14] T. Marilier and J.A. Richard. Non-linear mechanic and electric behavior of a robot axis with a harmonic-drive gear. *Robotics and Computer-Integrated Manufacturing*, 5(2/3):129–136, 1989.

[15] W. Seyfferth, A.J. Maghzal, and J. Angeles. Nonlinear modeling and parameter identification of harmonic drive robotic transmissions. *Proceeding of IEEE International Conference on Robotics and Automation*, 3:3027–3032, 1995.

[16] S.A. Shuvalov. Calculation of forces acting on members of a harmonic gear drive. *Russian Engineering Journal*, 59(10):5–9, 1979.

[17] Hamid D. Taghirad. *Robust torque control of harmonic drive systems*. PhD thesis, McGill University, March 1997.

[18] H.D. Taghirad. On the modelling and identification of harmonic drive system. Technical Report TR-CIM-97-02, Centre for Intelligent Machines, McGill University, January 1997.

[19] H.D. Taghirad and P.R. Belanger. Intelligent torque sensing and robust torque control of harmonic drive under free–motion. *Proceeding of IEEE International Conference on Robotics and Automation*, 2:1749–54, April 1997.

[20] H.D. Taghirad and P.R. Belanger. Robust torque control of harmonic drive under constrained motion. *Proceeding of IEEE International Conference on Robotics and Automation*, 1:248–253, April 1997.

[21] H.D. Taghirad, A. Helmy, and P.R. Belanger. Intelligent built-in torque sensor for harmonic drive system. *Proceedings of the 1997 IEEE Instrumentation and Measurement Technology Conference*, 1:969–974, May 1997.

[22] D.C. Threlfall. The inclusion of coulomb friction in mechanisms programs with particular reference to DRAM. *Mech. and Mach. Theory*, 13:475–483, 1978.

[23] A. Tustin. The effects of backlash and speed-dependent friction on the stability of closed-cycle control systems. *J. Inst. Elec. Eng.*, 94(2A):143–151, 1947.

[24] T.D. Tuttle and W.P. Seering. A nonlinear model of a harmonic drive gear transmission. *IEEE Transaction on Robotics and Automation*, 12(3):368–374, June 1996.

[25] D.P. Volkov and Y.N. Zubkov. Vibration in a drive with harmonic gear transmission. *Russian Engineering Journal*, 58(5):17–21, 1978.